Velocity correlations in granular materials

Tong Zhou
The James Franck Institute, The University of Chicago, 5640 South Ellis Avenue, Chicago, Illinois 60637
(Received 10 June 1998)

A system of inelastic hard disks in a thin pipe capped by hot walls is studied with the aim of investigating velocity correlations between particles. Two effects lead to such correlations: inelastic collisions help to build localized correlations, while momentum conservation and diffusion produce long ranged correlations. In the quasielastic limit, the velocity correlation is weak, but it is still important since it is of the same order as the deviation from uniformity. For systems with stronger inelasticity, the pipe contains a clump of particles in highly correlated motion. A theory with empirical parameters is developed. This theory is composed of equations similar to the usual hydrodynamic laws of conservation of particles, energy, and momentum. Numerical results show that the theory describes the dynamics satisfactorily in the quasielastic limit, though only qualitatively for stronger inelasticity. [S1063-651X(98)06512-X]

PACS number(s): 81.05.Rm, 05.20.Dd, 47.50.+d

I. INTRODUCTION

A granular system normally consists of a large number of particles colliding with one another and losing a little energy in each collision. If such a system is shaken to keep it in motion, its dynamics resembles that of fluids, in that the grains move seemingly randomly. Considerable effort has been devoted to the development of a continuum description for hydrodynamic equations [1–16].

Two approaches are employed by different authors. One is to set up a Boltzmann equation [1–5], and then to calculate hydrodynamic quantities by doing averaging with the distribution function derived from the equation. In this case, the molecular chaos assumption of the Boltzmann equation assumes zero correlations between particles. The other approach is to specify some hydrodynamic quantities, and then write down the conservation equations for them [6–16]. Generally, there are three equations: conservation of mass, balance of energy, and conservation of momentum. The mass conservation is in the standard hydrodynamic form. The momentum flux balance equation is in the form of Navier-Stokes equation for fluid dynamics. The energy ''conservation'' equation includes dissipation of energy via collisions.

The failing of Liouville's theorem for granular systems [17] casts doubts on the applicability of conventional approaches to hydrodynamic equations. Instead of writing down such equations based on unjustified assumptions, studying the dynamics with as few assumptions as possible, and trying to develop a theory closely connected to experiments, may be a less ambitious, but more solid approach.

One major consequence of the usual hydrodynamic theories of fluids is the Maxwell-Boltzmann distribution. In the frame in which the average system velocity is zero, this distribution implies no momentum correlations whatsoever among different particles. This result is true for classical elastic particles independently of the strength of the interparticle potential. In contrast, however, granular materials commonly induce correlated collective behaviors. Think about the surface waves of vibrated sand [18], or their convection patterns [19] (for a recent review, see Ref. [20].) The grains which take part in these collective behaviors do have correlated velocities. We therefore ask: how important are these correlations and how are they built up?

In this paper, we investigate the building up of correlations between velocities of grains. There are two mechanisms upon which correlations can be built up. One mechanism is due to the inelastic collisions between particles—after a collision, the velocity difference between two particles is smaller than that before the collision. This is a local effect, and the correlation is short ranged. The other mechanism is from momentum conservation—the larger the scale of a perturbation producing a localized average velocity, the slower the perturbation decays [21]. Fluctuations make the system nonuniform, so that there are localized clusters of particles all moving with about the same velocity. This correlation effect is a result of fluctuations which are neglected in the usual hydrodynamic treatments.

There are hydrodynamic theories ignoring fluctuations which are consistent with numerical results for weak inelasticities, but are quite inaccurate when inelasticities are strong, see, e.g., Ref. [22]. These theories are attempts to describe velocity fluctuations about some mean flow. They work fine in the quasielastic regime because correlations are small and negligible. But when inelasticities are strong, collisions can bring groups of neighboring particles to essentially the same velocity, and thereby produce a correlated motion which enhances the observable effect of any fluctuations in the system. We shall see this happen in our study.

The boundary conditions and system sizes independence of the essential characteristics of thermodynamic systems is one indication that thermodynamics is a universal description. However, this independence is lost in granular systems. We show that a universal description may still exist for the unconserved modes of the dynamics.

II. THIN PIPE MODEL

A. System

To investigate the validity of a hydrodynamic description, we should study the simplest situation which can show hydrodynamic behavior. In the elastic case, one-dimensional systems have too many conservation laws and do not show a fully ergodic or hydrodynamic behavior [2,23]. Here, we in-

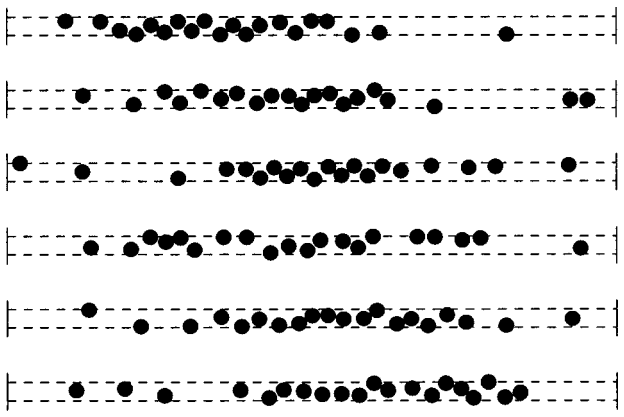

FIG. 1. Snapshots of the thin pipe system. The periodic side walls are indicated by dashed lines. The two end walls are energy sources kept at the same temperature. Notice how most of the particles fall into a cluster, which moves up and back through the system.

vestigate a two-dimensional system in the form of a long thin pipe (Fig. 1). The grains confined in the pipe are all identical, and the width of the pipe is set so that two grains cannot pass each other. Thus the motion of grains is two dimensional to ensure ergodicity, while at the same time we can order these grains. Pipe systems were studied before [24]. However, the no-passing condition enable this thin pipe model to simplify greatly both numerical and analytical calculations. (A two-dimensional version of this model was studied by Brey and Cubero [4].)

The two side walls are periodic—after leaving one side wall a particle comes back through the other. The distance between the side walls is chosen to be 2.5 times the radius of a particle. This choice prevents any passing. Two end walls are energy sources, and are kept at the same temperature.

For a thermodynamic system, the bulk properties should not depend on the details of boundary conditions. However, for some granular properties, boundary conditions can be quite important [2,19]. We employ two different boundary conditions in the numerical calculations: In both cases, when a particle hits an end wall the direction of its motion is turned around, and the particle is returned to the system. In the *fixed speed* boundary condition, the returned particles move away from the wall with a unit speed. Alternatively, in the *Boltzmann* boundary condition the returning speed is picked from a distribution $P(u)=2ue^{-u^2}$ [2]. All figures describe simulations with the Boltzmann boundary conditions unless otherwise specified.

B. Parameters and variables

We use the simplest model: nonrotating particles. After a collision, the radial relative velocity changes sign, and decreases by a factor of the restitution coefficient r, with $0<r<1$. In the collision, the other components of the velocities are unchanged. Thus $r=1$ is for elastic particles, and $r=0$ for extremely inelastic particles. We also define $\epsilon\equiv 1-r$.

The coordinate in the problem is an index, i, which indicates the position of the particle. Suppose there are $N=2n$ particles in the thin pipe. They are ordered as

$$-n,-(n-1),\ldots,-1,0,1,\ldots,(n-1).$$

By using the particle number i as our coordinate, we take advantage of the ''no-passing'' property of the thin pipe, and thereby obtain a Lagrangian description of the system.

Let us denote the velocity of the ith particle as $\vec{u}_i$, the relative velocity between the ith and $(i+1)$th particles as $\vec{v}_i\equiv\vec{u}_{i+1}-\vec{u}_i$, the velocity of the center of mass as $\vec{u}$, and the velocity of the ith particle with respect to the center of mass as $\vec{u}_i^r\equiv\vec{u}_i-\vec{u}$. Let us assume that the pipe is along the x direction. Then the x component of the velocities is special, and we denote the velocities as u_i and v_i. We use an overline notation to indicate the root mean square (rms) value of some quantities.

We propose a method to calculate profiles of various quantities throughout the system and the velocity correlations. (A *profile* is a plot of the value of some averaged quantity as a function of the particle number variable i.) Instead of the strongly correlated velocities $\vec{u}$'s, we study the relative velocities of neighboring particles, $\vec{v}$'s. In using $\vec{v}$ we focus our attention on the relative motion of the particles and away from their collective and correlated motion.

There are four parameters that will describe our system; the particle number N, the pipe length L, the width W, and the inelasticity ϵ. Of course ϵ measures the total amount of inelasticity in one collision. In a system with many particles, the effect of the inelasticity is enhanced by the correlation effects. For this reason, we expect two combinations of N and ϵ to be important. The product $N\epsilon$ measures the total amount of inelasticity in the system. For a one-dimensional system, imagine a particle with a large velocity hitting a group of n particles, sitting almost at rest. The added momentum will cascade down the group until at the end of the line the transmitted momentum will be diminished by a factor $\exp(-n\epsilon)$. In addition, a previous calculation [12] showed that dissipation of energy led to a gradual decay of temperature in the form of an exponential of $-c\sqrt{\epsilon}n$, where c is a constant. Thus we expect a dip in temperature determined by the combination of parameters $\sqrt{\epsilon}N$. Changing the remaining parameters L and W will only modify some numerical factors in the theory—but will not change the qualitative behavior of the system.

The system shown in Fig. 1 contains both low density and intermediate density regimes. There are some complication in such systems because of different geometrical factors for different density regimes [12]. To avoid such complication and focus on the dynamics of the system, we carry out our numerical calculations only for systems with extremely high density, where the typical spacing between neighboring particles is about 2% of the radius of a particle; or for systems with extremely low density, where the spacing at the highest density region of the system is about ten times the radius. The essential characteristics of the dynamics are independent of density regimes.

C. Steady state

This system can reach a statistical steady state. In this state, the particles move fast near the hot walls, and the density is low there. Toward the center of the system, the density

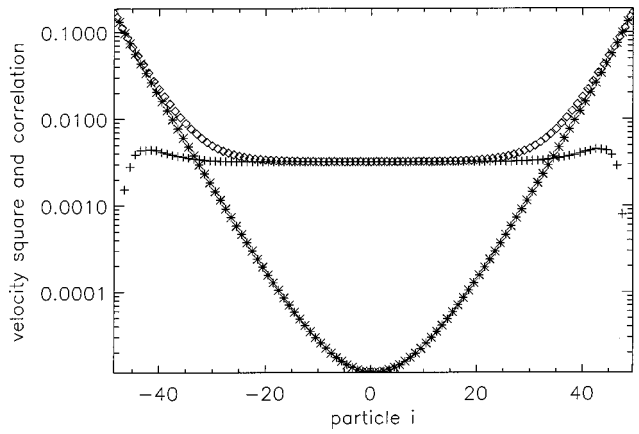

FIG. 2. Profiles of a low density system of 100 particles with $r=0.94$, just above the critical value for inelastic collapse r_c. $\diamond$ is for $\langle u_i^2\rangle$, $*$ for $\langle v_i^2/2\rangle$, and $+$ for $\langle u_i u_{i+1}\rangle$.

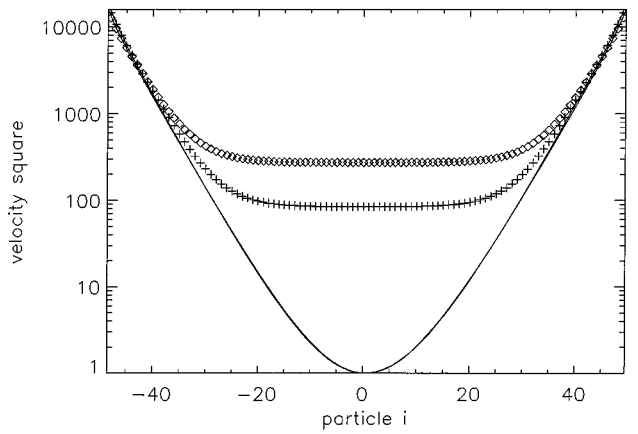

FIG. 3. Profiles of $\langle v_i^2/2\rangle$ and $\langle u_i^2\rangle$ for two different boundary conditions. The system has low density 100 particles and $r=0.94$. Each profile is rescaled by changing the scale of velocity so that $\langle v_0^2/2\rangle=1$. There are two lines, which nearly overlap each other, describing $\langle v_i^2/2\rangle$. $\diamond$ is for $\langle u_i^2\rangle$ with the *Boltzmann* boundary condition, and $+$ is for $\langle u_i^2\rangle$ with a *fixed speed* boundary condition. These two profiles are very different.

is higher. For quasielastic situations, the system is relatively uniform; however for stronger inelasticities, the particles near the center can form a cluster and move with about the same velocity. The cluster was seen and understood in previous calculations [12,21]. The relative motion of particles is reduced by the inelastic collisions between them. In fact, when $N\epsilon$ is large, the relative motion can be very small and then momentum conservation causes each particle in the cluster to have about the same velocity, which is just the mean velocity of the cluster.

Figure 2 shows a plot of some profiles in an inelastic situation with two hot walls. Notice that the profile of $\langle u_i^2\rangle$ has a flat region at the center. This was seen before [4]. That flattening occurs because the central particles almost always fall within a cluster, and the cluster moves with a large average velocity but small relative velocities. [The fluctuation velocities (see below) vary on a very small time-scale, whereas the correlated motion (cluster moves from one wall to the other) varies on a much longer time scale. The averages are taken over even longer times.] The plot of $\langle v_i^2\rangle$ indeed shows that the relative velocity decreases to a very small value near the center of the system. This decay in $\langle v_i^2\rangle$ is roughly what we might expect from a simple hydrodynamic description, in which one balances energy flux with dissipation [12]. The hydrodynamics then gives an i dependence which is a superposition of growing and decaying exponentials. That theory is in some sense a mean field theory which ignores the correlations between velocities. In much of what we do, delicate and long range correlations effects will be very important for the behavior of $\vec{u}$'s but less important for the $\vec{v}$'s. In fact we shall see that the rms of v_i obeys

$$\frac{\partial^2}{\partial i^2}\overline{v_i}=b^2\overline{v_i}, \tag{1}$$

where b^2 is proportional to ϵ for small values of the inelasticity. The solution to the equation is

$$\overline{v_i}=\overline{v_0}\cosh(bi). \tag{2}$$

Equations (1) and (2) describe a situation in which heat conduction balances against energy dissipation.

On the other hand, the large degree of correlation between u_i and u_{i+1} is quite unexpected. No such correlation occurs in the usual statistical mechanics. This kind of correlation effect is not directly contained in any hydrodynamic equations. As we shall see, it is a result of fluctuations not usually included in hydrodynamics.

Boundary conditions are often important for granular systems. Figure 3 shows the effects of boundary conditions. We see $\langle u_i^2\rangle$ depends sensitively on boundary conditions. In contrast, after a rescaling, $\langle v_i^2\rangle$ is nearly independent of boundary conditions. There is no similar rescaling which can make the profiles for $\langle u_i^2\rangle$ overlap.

D. Correlated motion and random motion

Since

$$\langle v_i^2\rangle=\langle u_i^2+u_{i+1}^2\rangle-2\langle u_i u_{i+1}\rangle, \tag{3}$$

when the correlation $\langle u_i u_{i+1}\rangle$ is weak, we simply have $\overline{v_i^2}=2\overline{u_i^2}$ (an overline notation is to indicate the *rms* value of some quantities), assuming a weak i dependence. But when correlation is strong, the relation between $\overline{v_i^2}$ and $\overline{u_i^2}$ is quite different. We shall study that difference in detail. From the mechanism described above, we know that, near the center, $\overline{u_i^2}$ is roughly constant, independent of i, as a consequence of the motion of the cluster. Conversely, $\overline{v_i^2}$ will vary because of energy dissipation. In our considerations, we shall focus upon v_i^2, which has an average which can be interpreted as a local temperature. We argue that v_i^2 is a more relevant variable than u_i^2, since, to a large extent, it determines the collision rate, and the effect of a collision. In addition, $\overline{v_i}$ behaves as predicted by the simple hydrodynamics theory, it

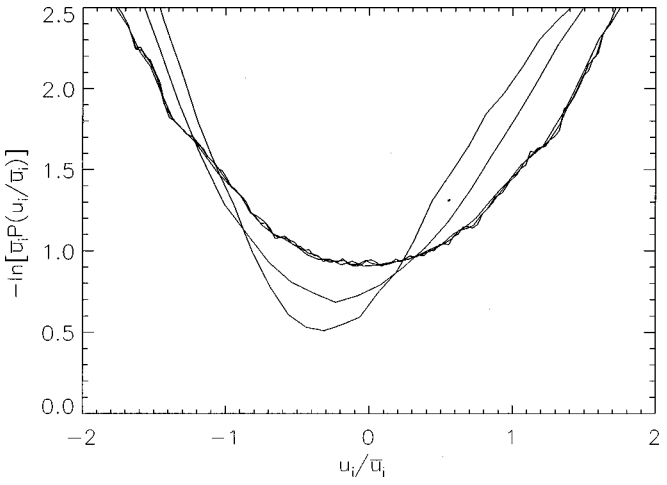

FIG. 4. Time-average probability for u_i in a low density system with $N=100$ and $r=0.94$. Five such curves are shown, for $i=0$, $-10,-20,-35$, and -45. The first three in this list are close to Gaussian, and they lie almost on top of one another. The other two are quite different.

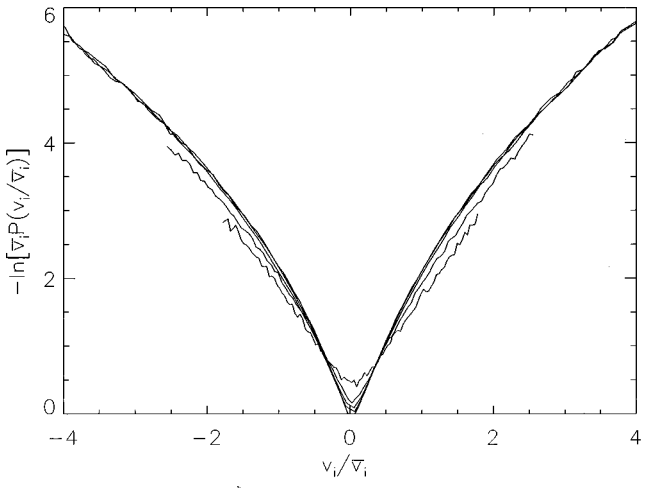

FIG. 5. Probability distribution for relative velocities. The calculation is done as a time average for a low density system with $N=100$, $r=0.94$ and $i=0,-10,-20,-35$, and -45. The PDF's for v_i's collapse into a single curve after a rescaling. Once again the three curves for particles inside the cluster fall on top of one another, while the others are slightly different.

decays exponentially, and forms a hyperbolic cosine curve as a function of i. Conversely, $\overline{u_i}$ is produced by subtle correlation effects.

We can also write Eq. (3) in the form

$$\tfrac{1}{2}\langle u_i^2+u_{i+1}^2\rangle=\tfrac{1}{2}\langle v_i^2\rangle+\langle u_i u_{i+1}\rangle. \tag{4}$$

The term on the left hand side describes the total motion with respect to the lab frame, the second term on the right hand side describes the correlated motion between particle i and particle $i+1$, and the first term on the right hand side describes the random relative motion between neighboring particles. Put into words,

$$(\text{total motion})=(\text{random motion})+(\text{correlated motion}).$$

The first term on the right can be interpreted as a temperature; the second as a result of the correlated motion of the two particles. In this way, we see that the ratio

$$R_i=\frac{\langle v_i^2\rangle}{\langle u_i^2+u_{i+1}^2\rangle}=\frac{(\text{random motion})}{(\text{total motion})} \tag{5}$$

indicates the amount of correlation in the motion. When the inelasticity is weak, the velocity correlations are also weak, and this ratio is very close to unity. For strong inelasticity, where correlations are strong, this ratio can be very small.

E. PDF's of velocities

The probability distribution functions (PDF's) for u_i and v_i provide considerable additional insight into the nature of the system. See Figs. 4 and 5. In these figures, the variables are normalized to give each PDF the same variance.

In the PDF plots for u_i, we see a fundamentally Gaussian behavior inside the cluster. Outside the cluster, the part of the curve shown is Gaussian but there is a strong high velocity tail.

In contrast, the PDF plots for v_i show a structure which is essentially the same inside and outside the cluster. Thus, all over the system, the $v's$ behave in the same way, but this behavior is quite nontrivial. We will use the constancy of the PDF of v_i (in the whole system) and u_i (in the interior of the system) to develop our theoretical model.

III. MOTION IN THE CENTER OF MASS FRAME

Figure 3 suggests that we can decompose the dynamics of the system into two parts: (I) the motion of grains in the center of mass frame, and (II) the motion of the center of mass itself. Part I is independent of boundary conditions and all the effects of boundary conditions are attributed to part II. Part I is described in terms of the variables $\vec{v}_i$ which may be considered to be weakly correlated with one another. Part II involves variables $\vec{u}_i$, and strong correlations among the variables. In this section, we focus our attention upon the effects of conservation laws upon the system, and particularly on the motion of part I.

A. Theoretical calculation

Since the number of degrees of freedom of part I is equal to the number of $\vec{v}_i$'s, this part of motion can be described in terms of $\vec{v}_i$'s. So the problem can be solved in two steps: the rms of $\vec{v}_i$ and the correlations between $\vec{v}_i$'s. Our interest in the variable $\vec{v}_i$ is also based on the numerical results shown in Sec. II that the profile of $\overline{v_i}$ is, in accordance with hydrodynamics theory and Eq. (2), a hyperbolic cosine function of i, plus its weak dependence on the boundary conditions—these suggest that $\vec{v}_i$ can form the basis of a solution to some simple hydrodynamics equations.

1. Profile of $\overline{v_i}$

Collisions. For the steady state, mass conservation is reduced to trivial statements that $\langle\vec{u}_i\rangle=0$ and $\langle\vec{v}_i\rangle=0$. The momentum and energy transfer between particles are results

of collisions between them. So to investigate momentum and energy conservation, we study the effects of a single collision first.

Let us consider a collision between the ith and $(i+1)$th particles, during which $\vec{u}_i$, $\vec{u}_{i+1}$, and $\vec{v}_i$ change to $\vec{u}_i'$, $\vec{u}_{i+1}'$, and $\vec{v}_i'$, respectively. According to the inelastic collision rule,

$$\vec{u}_i' = \vec{u}_i + \frac{1+r}{2}\hat{n}v_{i,n}, \tag{6}$$

$$\vec{u}_{i+1}' = \vec{u}_{i+1} - \frac{1+r}{2}\hat{n}v_{i,n}, \tag{7}$$

$$\vec{v}_i' = \vec{v}_i - (1+r)\hat{n}v_{i,n}, \tag{8}$$

where $\hat{n}$ denotes a unit vector, pointing in the direction of the line of centers at the point of collision while $v_{i,n}$ is the component of $\vec{v}_i$ in that direction.

Pressure. The collision described above results in a change in the momentum of particle $i+1$,

$$\vec{u}_{i+1}' - \vec{u}_{i+1} = -\frac{1+r}{2}\hat{n}v_{i,n}.$$

In a long time interval t, the momentum change of particle $i+1$ from collisions between particle i and particle $i+1$ is

$$P_i W t = -\frac{1+r}{2}\sum^{(i)} (\hat{n}\cdot\hat{x})v_{i,n}, \tag{9}$$

where $\Sigma^{(i)}(\cdots)$ is the summation over all the collisions between the ith and $(i+1)$th particles. The x component in Eq. (9) is the direction along the pipe.

In writing Eq. (9), we identified the rate of momentum transfer from particle i to particle $i+1$ as an average pressure, P_i times the pipe width W, while t is the time for the summation. We shall be dealing a lot with sums over collisions as in equation (9). To understand them, we should realize that $\Sigma^{(i)}(\cdots)/t$ can be written as the rate of collisions between i and $i+1$, c_i, times an average over collisions $\langle\cdots\rangle_i$ of this type. Notice that the average over collisions is very different from the time-average $\langle\cdots\rangle$. For example, $\langle v_i\rangle$ must be zero in any steady state situation. However, since v_i must be negative for a collision to occur, then $\langle v_i\rangle_i$ must be negative.

Now go back to Eq. (9). For the steady state, the momentum flux must be a constant, so this summation over a long time interval must be independent of i. Thus the momentum conservation law has the consequence that the pressure, as defined by Eq. (9), is independent of i. So the equation for momentum conservation in our system takes the form

$$-\frac{1+r}{2Wt}\sum^{(i)} (\hat{n}\cdot\hat{x})v_{i,n} = -\frac{1+r}{2W}c_i\langle(\hat{n}\cdot\hat{x})v_{i,n}\rangle_i = P. \tag{10}$$

The distribution functions for relative velocity depend only weakly on i (Fig. 5). Thus all components and averages of $\vec{v}_i$ vary in proportion to one another as i is varied. As i approaches the center of the system, the typical value of the momentum transfer per collision declines in proportion to $\overline{v_i}$. Then, by Eq. (10), the collision rate increases by going inversely as the relative velocity.

Using the same arguments, we can also understand the pressure definition [Eq. (10)] in a familiar form. Pressure is a flow of momentum per unity area per unit time. One kind of flow involves transfer of momentum from the ith particle to the next one. The collision rate is of the order of $\overline{v_i}/l_i$, where l_i is the mean spacing between the two particles. During each collision, the average momentum transfer is proportional to $\overline{v_i}$. From these two facts, the momentum flux is proportional to $\overline{v_i^2}/l_i$. The average of relative velocity squared is the temperature T, while $1/(Wl_i)$ is the density ρ. This result is then in the familiar form $P=\rho T$. This identification is an order of magnitude argument. For calculations, we use the exact result [Eq. (10)].

Energy balance. Now let us study the effects of this collision on the energy balance. The energy transfers to particle i and particle $i+1$ are, respectively,

$$\vec{u}_i'^2 - \vec{u}_i^2 = \frac{1+r}{2}(u_{i+1,n}^2 - u_{i,n}^2) - \frac{1-r^2}{4}v_{i,n}^2,$$

$$\vec{u}_{i+1}'^2 - \vec{u}_{i+1}^2 = \frac{1+r}{2}(u_{i,n}^2 - u_{i+1,n}^2) - \frac{1-r^2}{4}v_{i,n}^2,$$

and the energy dissipation is

$$[(\vec{u}_i^2 + \vec{u}_{i+1}^2) - (\vec{u}_i'^2 + \vec{u}_{i+1}'^2)] = \frac{1-r^2}{2}v_{i,n}^2.$$

We can form an energy conservation equation by balancing the energy dissipation with the difference of the energy flux. However, the above expressions involve $\vec{u}_i$'s which are correlated and do not belong to the motion in the center of mass frame. To find a consistent description, we want to express this conservation in terms of $\vec{v}_i$'s. Because the essential dynamic process is determined by the collision rule, Eqs. (6)–(8), an equation describing the balance of a quadratic form of $\vec{v}_i$'s will incorporate the energy conservation.

In fact, we have, from Eqs. (6)–(8),

$$\vec{v}_i'^2 - \vec{v}_i^2 = -(1-r^2)v_{i,n}^2,$$

$$\vec{v}_{i+1}'^2 - \vec{v}_{i+1}^2 = (1+r)v_{i,n}v_{i+1,n} + \frac{(1+r)^2}{4}v_{i,n}^2,$$

$$\vec{v}_{i-1}'^2 - \vec{v}_{i-1}^2 = (1+r)v_{i,n}v_{i-1,n} + \frac{(1+r)^2}{4}v_{i,n}^2.$$

For the steady state, the total change in v_i^2 should vanish,

$$\sum^{(i)} (\vec{v}_i'^2 - \vec{v}_i^2) + \sum^{(i+1)} (\vec{v}_i'^2 - \vec{v}_i^2) + \sum^{(i-1)} (\vec{v}_i'^2 - \vec{v}_i^2) = 0,$$

or, equivalently,

$$-(1-r)\sum^{(i)} v_{i,n}^2+\sum^{(i+1)}\left(v_{i,n}v_{i+1,n}+\frac{1+r}{4}v_{i+1,n}^2\right)+\sum^{(i-1)}\left(v_{i,n}v_{i-1,n}+\frac{1+r}{4}v_{i-1,n}^2\right)=0. \tag{11}$$

The first term is from energy dissipation, while the other terms take the form of energy transfer.

Profile of $\overline{v_i}$. We wish to simplify our energy-flow equation by reducing it to an equation for $\langle v_{i,n}^2\rangle_i$. However, correlations between $\vec{v}_i$ and $\vec{v}_{i+1}$ appear in Eq. (11). We must eliminate these terms. For an elastic uniform system, this correlation takes a simple form

$$\begin{aligned}\langle v_i v_{i+1}\rangle&=\langle (u_{i+1}-u_i)(u_{i+2}-u_{i+1})\rangle\\&=-\langle u_{i+1}^2\rangle\\&=-\tfrac{1}{2}\overline{v}_i\overline{v}_{i+1}.\end{aligned} \tag{12}$$

In the elastic case, it is equally true, for the usual time-weighted average or for the collision weighted average, that

$$\sum^{(i+1)}(v_{i,n}v_{i+1,n})+\sum^{(i-1)}(v_{i,n}v_{i-1,n})=-\tfrac{1}{2}(n_{i+1}^c v_i^c v_{i+1}^c+n_{i-1}^c v_i^c v_{i-1}^c), \tag{13}$$

where $v_i^c\equiv\sqrt{\Sigma^{(i)}\vec{v}_{i,n}^2/n_i^c}$, and n_i^c is the total number of collisions between particle i and particle $i+1$, $n_i^c=c_i t$. As defined here, v_i^c is a collision average of $\vec{v}_i$ just before collisions.

Equation (13) has scalars on the left and right hand sides. There are corrections to this relation for inelastic particles and when there is a spatial variation in the averages. The corrections must be scalars and of order $\overline{v_i^2}$. One correction is of the order of $\epsilon\overline{v_i^2}$. In the other correction, d^2/di^2 is applied to $\overline{v_i^2}$. However, in virtue of the result in Eq. (1), these two terms are really the same. Consequently, we need only one of these two corrections. We write the resulting structure, in an even parity form, as

$$\sum^{(i+1)}(v_{i,n}v_{i+1,n})+\sum^{(i-1)}(v_{i,n}v_{i-1,n})=-\frac{1-a_1\epsilon}{2}(n_{i+1}^c v_i^c v_{i+1}^c+n_{i-1}^c v_i^c v_{i-1}^c). \tag{14}$$

Now Eq. (14) can be used to transform Eq. (11) into the form

$$-\epsilon n_i^c v_i^{c2}+\frac{1+r}{4}(n_{i+1}^c {v_{i+1}^c}^2+n_{i-1}^c {v_{i-1}^c}^2)-\frac{1-a_1\epsilon}{2}(n_{i+1}^c v_i^c v_{i+1}^c+n_{i-1}^c v_i^c v_{i-1}^c)=0,$$

or, since $n_i^c v_i^c$ is a constant independent of i [see Eq. (10)], we find a heat flow equation

$$(6-4a_1)\frac{\epsilon}{1+r}\overline{v}_i=\overline{v}_{i+1}-2\overline{v}_i+\overline{v}_{i-1}.$$

In writing the last structure we noticed that different kinds of collision averages all have the same i dependence. Now we can phrase our result in a continuum form

$$(6-4a_1)\frac{\epsilon}{1+r}\overline{v}_i=\frac{d^2\overline{v}_i}{di^2}.$$

In this way, we obtain

$$\overline{v}_i=\overline{v}_0\cosh(bi), \tag{15}$$

where

$$b^2=(3-2a_1)\epsilon. \tag{16}$$

2. Correlations between velocities

Correlations between v_i's are short ranged. Let us only consider the nearest neighbor correlation. When there is no dissipation, the only nonvanishing correlation of the v_i's is the nearest neighbor average of Eq. (12). For $r<1$, there is a small correction to that relation. Just as before [see Eq. (14)], we write an equation for the average of a nearest neighbor product in the same form as in the elastic case, but with a correction proportional to ϵ,

$$\langle v_i v_{i+1}\rangle=-\frac{1-a_2\epsilon}{2}\overline{v}_i\overline{v}_{i+1}, \tag{17}$$

where the averages are time averages.

This assumption, with the profile of $\overline{v_i}$ determined above, completes a description of the motion of grains in the center of mass of frame, i.e., part I of the dynamics described before. As an example, let us calculate the correlations between u_i^r's, the velocities of particles in the center of mass frame. To illustrate the similarity between this part of the dynamics and conventional thermodynamics, i.e., the independence of boundary conditions and system sizes, we consider the center of mass frame of the $2m$ particles at the center of the system. Keep in mind that rather than fixed, m can be treated as a variable in the following calculation.

Express u_i^r in terms of v_i's,

$$u_i^r=-\frac{1}{2m}\left[\sum_{j=i}^{m-1}(m-j)v_j-\sum_{j=-(m-1)}^{i-1}(m+j)v_j\right].$$

So

$$\frac{2u_i^r u_{i+1}^r}{u_i^{r2}+{u_{i+1}^r}^2}=\frac{A-m^2v_i^2}{A+m^2v_i^2},$$

where

$$A=\left[\sum_{j=i+1}^{m-1}(m-j)v_j-\sum_{j=-(m-1)}^{i-1}(m+j)v_j-iv_i\right]^2.$$

Let us calculate the correlation between u_0^r and u_1^r. Keeping only the correlations between nearest neighbor, we have

$$\left\langle \left[\sum_{j=1}^{m-1} (m-j)v_j - \sum_{j=-(m-1)}^{-1} (m+j)v_j \right]^2 \right\rangle = 2\left\langle \sum_{j=1}^{m-1} (m-j)^2 v_j^2 + 2\sum_{j=1}^{m-2} (m-j)(m-j-1)v_j v_{j+1} \right\rangle$$

$$= (m-1)^2\overline{v_1^2} + \overline{v_{m-1}^2} + \sum_{j=1}^{m-2} [(m-j)\overline{v_j} - (m-j-1)\overline{v_{j+1}}]^2$$

$$+ 2a_2\epsilon \sum_{j=1}^{m-2} (m-j)(m-j-1)\overline{v_j}\,\overline{v_{j+1}}$$

$$\equiv A_1\overline{v_0^2},$$

so

$$\frac{\langle 2u_0^r u_1^r \rangle}{\langle u_0^{r2} + u_1^{r2} \rangle} = \frac{A_1 - m^2}{A_1 + m^2}. \tag{18}$$

Obviously, when $m=1$, the above ratio is -1, because $u_0^r = -u_1^r$ at all time. For elastic particles, the ratio can be calculated analytically to be $-1/(2m-1)$. The inelasticity changes this dependence. Let us call $2m$ the ''cluster size,'' since it corresponds to the usual practice of defining a cluster then separating the motion of particles into mean flow and fluctuations. From expression (18), we see that when the cluster is large enough, A_1 can be large comparing to m^2; then the correlations between velocity fluctuations can be large.

B. Numerical results

We carry out numerical simulations to investigate the statistical steady state of the system. Here we compare the numerical results with the above theory describing the motion in the center of mass frame.

1. Quasielastic situations

First let us look at the quasielastic situations, i.e., very small ϵ. Before testing the profile of v_i's, we exam the crucial assumption, Eq. (14).

Now let us look more sharply at the data. To find a_1, we do a very accurate determination of the ratio of averages from the left and the right hand sides of Eq. (14). This equation is then solved at each i value to find a local value of a_1. The result is shown in Fig. 6. The theory is right if a_1 is independent of i, and wrong if it has an important i dependence. The figure seems to show that there is an excellent fit for the smaller value of ϵ, and a bad fit for the larger.

From Eq. (16) we see that the important combination determining the properties of the profile of $\overline{v}$ is $3-2a_1$. But a_1 is very close to 1.5, as shown in Fig. 6. Then the a_1 effect changes the prefactor in Eq. (16) from 3 to $3-2a_1$, i.e., by a factor of 50. The velocity correlations renormalize ϵ, and reduce the energy dissipation.

Also a_1 is essentially a local correlation effect originated from the inelastic collisions. For an elastic system with comparable inhomogeneity, there is also a correction to the factor $-\frac{1}{2}$ in Eq. (14), but the correction is usually an order of magnitude smaller than the effects we are seeing here.

A test of Eq. (15) is shown in Fig. 7. Analysis like this permits the determination of the slope like the one in Fig. 7 as a function of ϵ. We have called this slope b. Figure 8 shows that the numerical values give an ϵ dependence for b which fully supports the theory. However, notice that all this analysis applies to very small values of ϵ. Section III B 2 considers more inelastic situations.

2. Stronger inelasticity regime

We look at smaller r's. To avoid inelastic collapses, we limit our r to be greater than r_c. For a system of 100 particles with extremely high density, $r_c \approx 0.95$.

When r becomes smaller, there is a cluster of particles moving around the center of the pipe, all with about the same velocity. The system is in a state far away from equilibrium. Also, it is very nonuniform—the particles around the center are highly correlated, while those near the boundaries move independently; the energy flux is strong near the end walls, but rather weak inside the system. As a consequence, the PDF's of quantities change significantly from particles near the center to those near the boundaries, e.g., the PDF's of u_i's, though there is no large change in the PDF's of v_i's.

Figure 9 once again plots a quantity which should be linear in i if the theory, Eqs. (15), is right. Now, for this larger value of ϵ, there are substantial variations in slope. It appears that the theory does not apply for the 15 particles nearest to

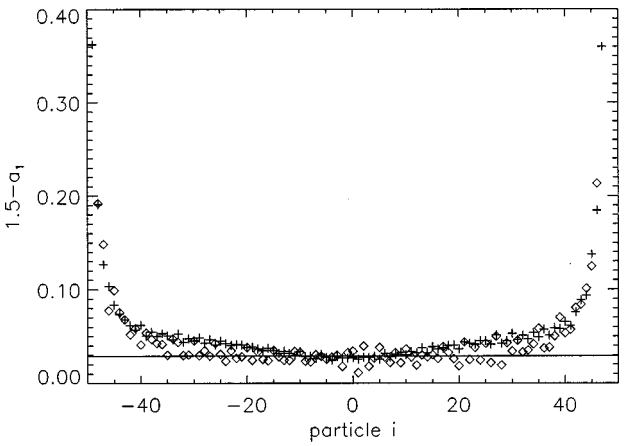

FIG. 6. Numerical results for $1.5-a_1$ for a high density system with 100 particles averaged over 2×10^9 collisions. a_1 is defined in Eq. (14). $\diamond$ is for $r=0.995$; $+$ is for $r=0.95$. The line is for $1.5-a_1=0.029$ from the fit in Fig. 8.

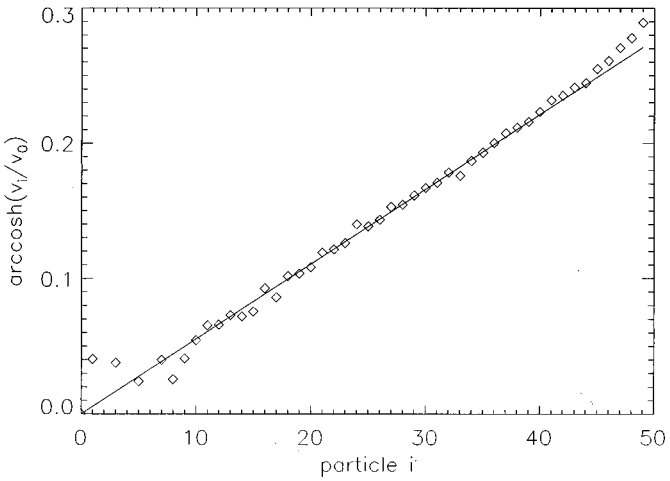

FIG. 7. Fit to a hyperbolic cosine curve of the profile of the $\overline{v_i}$ for a high density system of 100 particles and $r=0.9995$. To check Eq. (15), we take the inverse of the hyperbolic cosine of $\overline{v_i}/\overline{v_0}$ and plot the result as a function of i. The straight line indicates a fit to the theory. In the theory, the slope is proportional to the square root of ϵ. Here the slope is 0.0055, which is equal to the square root of 0.06ϵ.

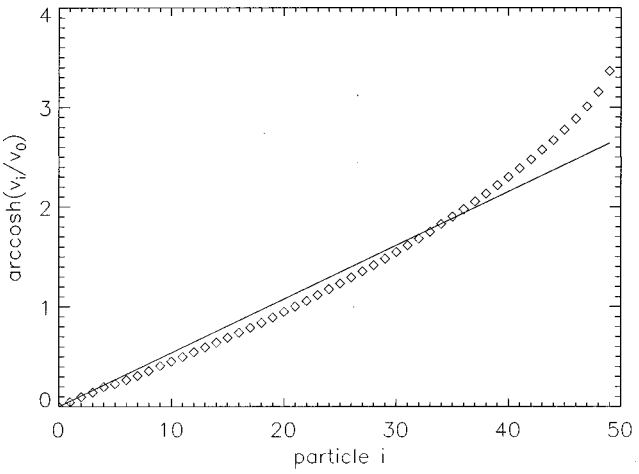

FIG. 9. Fit to a hyperbolic cosine curve of the profile of $\overline{v_i}$ for a high density system of 100 particles and $r=0.95$. This is a higher-ϵ analog of Fig. 7. The straight line corresponds to a hyperbolic cosine profile curve, and its slope is 0.054, a value extrapolated from the expression for quasielastic cases (Fig. 8). However, the straight-line fit is not very good, especially near the boundary.

each of the boundaries, and that it might have small troubles elsewhere. This discrepancy is also shown when we plot the slope, calculated from doing numerical derivatives on Fig. 9 to give b as a function of i. This plot is given as Fig. 10.

The discrepancy between the theory and numerical results for strong inelasticity is not surprising. Though taking into account the correlations between fluctuations, the theory is still based on concepts of conventional fluids—no internal structures are considered. However, when inelasticity is strong, the dynamics is affected by intrinsic structures of the collection of the particles, and the whole system may belong to a different phase [17]. A satisfactory theory must incorporate this feature.

Now let us look at the velocity correlations. Only the nearest neighbor correlation [Eq. (17)] is considered. The theory leads to expression (18) of the correlation between u_0^r and u_1^r, which is independent of system sizes or boundary conditions. To test this expression, we numerically calculate this correlation with respect to different cluster sizes, i.e., different m, with Eq. (18), and with the profile of $\overline{v_i}$ calculated numerically. The comparison between theory and numerical result is shown in Fig. 11. We see the correlation increases with increasing cluster size. The comparison is the best for $a_2=0.6$. When the cluster size is large enough, most of the total motion belongs to the correlated motion. We want to point out that this curve is independent of boundary conditions. Also for systems with different sizes, we obtain sections of different length from this same curve, as shown in the figure.

We want to point out that the major point of Fig. 11 is to demonstrate that part of the dynamics, the motion in the center of mass frame, is independent of boundary conditions and system sizes. The agreement between theory and numerical results can not be viewed as a strong support for the details of the theory because the profile of $\overline{v_i}$ is from numerical calculations, rather than Eq. (15); also, the value a_2

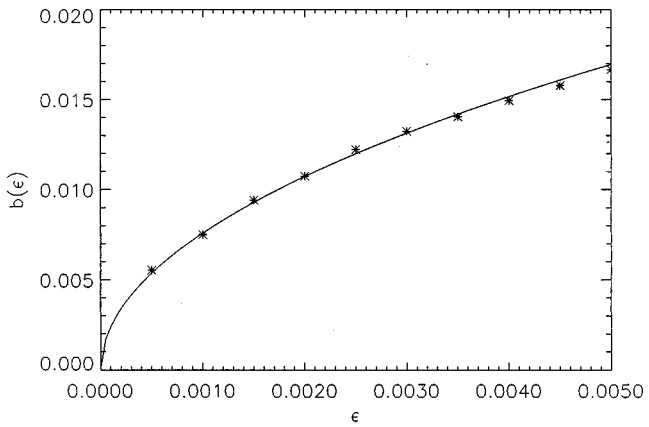

FIG. 8. The ϵ dependence of b for systems with $N=100$. The curve is the theoretical fit, the square root of 0.058ϵ. [See Eq. (15).]

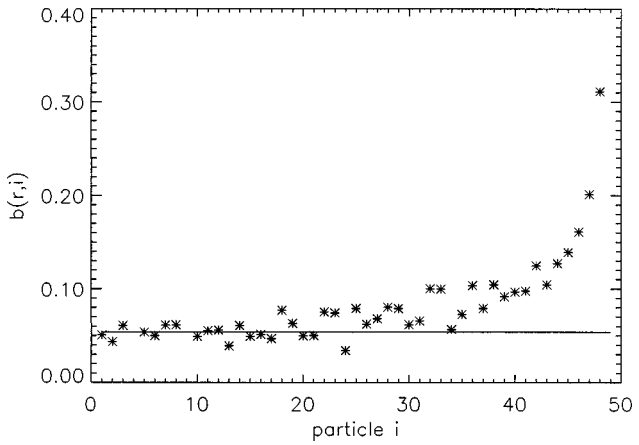

FIG. 10. The position dependence of the prefactor b in a high density system with 100 particles and $r=0.95$. The line is $b=0.054$, extrapolated from the quasielastic cases.

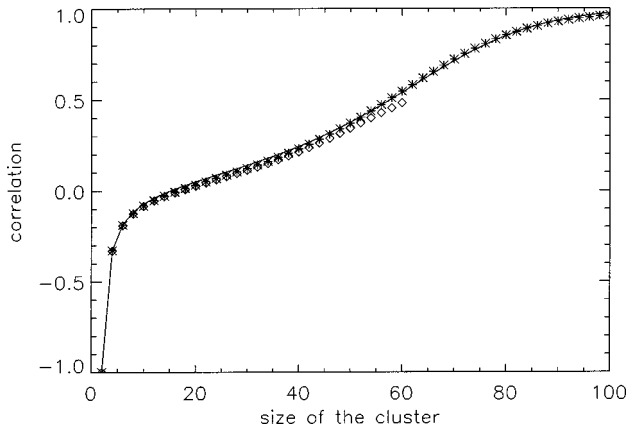

FIG. 11. The cluster size dependence of ratio (18). The system is in a low density regime, with $r=0.94$. * is from time average results of a simulation with 100 particles and ◇ is from a simulation with 60 particles. The curve is from Eq. (18) with $a_2=0.6$.

$=0.6$ is a fitting parameter. The theory captures some qualitative features of the dynamics, but is still incomplete.

IV. MOTION OF THE CENTER OF MASS

Because the total momentum of the system can be only changed by collisions between the outermost particles and the walls, and the motion of the outermost particles is close to that of an elastic system, the motion of the center of mass should also be close to that of an elastic system. For an elastic system,

$$\langle u^2\rangle=\left\langle\left(\sum_i u_i/N\right)^2\right\rangle=u^{*2}/N, \tag{19}$$

where u^* is the rms speed of the outermost particle. From Fig. 12 we see this estimate is about right, though the numerical factor must be calculated from detailed distributions. The result also seems sensitive to ϵ. This is because the PDF

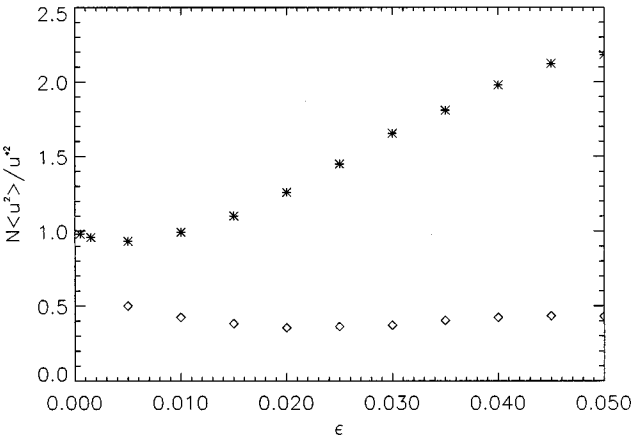

FIG. 12. Test of Eq. (19) for two boundary conditions for high density systems with $N=100$. The ratios are all around 1, as we expect from our order of magnitude argument. The * is for the Boltzmann boundary condition, and the ◇ is for the fixed speed condition. The motion of the center of mass depends strongly on the boundary conditions.

for the velocity of the outermost particle is more skewed for higher values of ϵ, and so the ratio between u^* and the momentum transferred into the system from the wall depends on ϵ. Notice that the motion of the center of mass depends strongly on the boundary condition.

Suppose the motion of particles in the center of mass frame is independent of the motion of the center of mass itself, i.e., u is uncorrelated to v_i's; then

$$\langle u_i^2\rangle=\langle u_i^{r2}\rangle+\langle u^2\rangle.$$

Simulations show that the profile of $\overline{v_i}$ is nearly independent of boundary conditions, and so is the motion of the system in the center of mass frame. However, $\langle u^2\rangle$ depends sensitively on the boundary conditions, and so does the motion of the particles in the lab frame, i.e., the profile of $\langle u_i^2\rangle$ (Fig. 3).

Due to the motion of the center of mass, correlations between u_i's are enhanced, comparing to those between u_i^r's:

$$\frac{\langle 2u_iu_{i+1}\rangle}{\langle u_i^2+u_{i+1}^2\rangle}=\frac{2\langle u_i^ru_{i+1}^r\rangle+2\langle u^2\rangle}{\langle u_i^{r2}+{u_{i+1}^r}^2\rangle+2\langle u^2\rangle}$$

or

$$\frac{v_i^2}{\langle u_i^2+u_{i+1}^2\rangle}=\frac{v_i^2}{\langle u_i^{r2}+{u_{i+1}^r}^2\rangle+2\langle u^2\rangle}=R_i. \tag{20}$$

The ratio R_i between random motion and total motion was defined by us in Eq. (5).

Behavior of the ratio R_0

When $n\epsilon$ is small, we can expand expression (20), using Eqs. (15), (18), and (19). Keeping terms linear in ϵ, we have

$$-\ln(R_0)=\frac{\epsilon}{2n}\{[(n-\alpha)^2+(n-1)](3-2a_1)+2(n-1)(n-2)a_2/3\}, \tag{21}$$

where $0<\alpha<1$. From Eq. (21) we see that when $n\epsilon$ is small, $-\ln(R_0)$ is proportional to $n\epsilon$.

Numerical results of $-\ln(R_0)$ are shown in Fig. 13. We do see that $-\ln(R_0)$ is proportional to ϵ for very small ϵ. However, when ϵ is large, where we expect strong nonlinear effects, it is proportional to ϵ^2.

As we argued in Sec. II, there are two important combinations of N and ϵ. The product $N\sqrt{\epsilon}$ describes how temperature decays toward the center of the system, which agrees excellently with the numerical results when ϵ is very small. However, Eq. (21) shows that in this limit, only the product $N\epsilon$ appears in the final expression for R_0. This seems to suggest that R_0, i.e., the degree of the coherence of the particles' motion, is determined by the product $N\epsilon$ (Figs. 14 and 15). These two figures exhibit rather interesting fea-

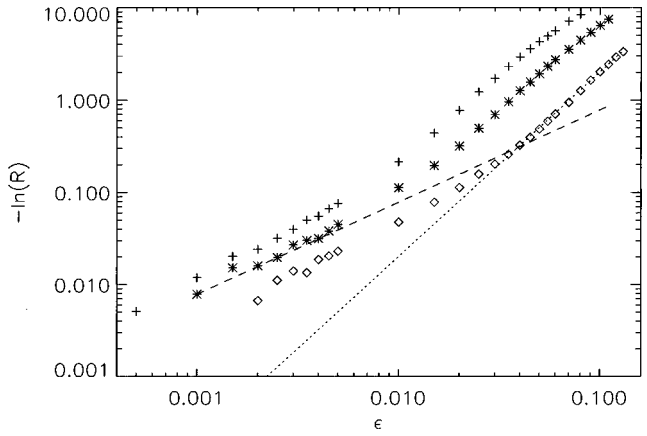

FIG. 13. The logarithm of ratio (5) for $i=0$ vs ϵ. + is for $N=100$, * is for $N=70$, and ◇ is for $N=40$. All three are for low density systems with the Boltzmann boundary condition. The dashed line indicates a dependence $\ln(R_0)\propto\epsilon$, and the dotted line indicates a dependence $\ln(R_0)\propto\epsilon^2$.

tures of the dynamics [25], though we do not have a satisfactory understanding of them.

V. CONCLUSION

In this paper, we investigated the steady state of a forced granular system in a thin pipe. Correlations between velocities of granular particles are shown to be important for a correct understanding of such systems. For systems in the quasielastic regime, correlation is small, but not negligible because the deviation from equilibrium is also small. (Correlation is usually ignored in this regime, see, for example, Ref. [6]. We have shown here that it cannot be ignored in a self-consistent theory.) For systems with stronger inelasticity, correlation is crucial for a correct theory. Our theory describes the dynamics satisfactorily in the quasielastic limit. For stronger inelasticities, numerical results show quite interesting behaviors of the system; however, our theoretical understanding is only qualitative at this stage.

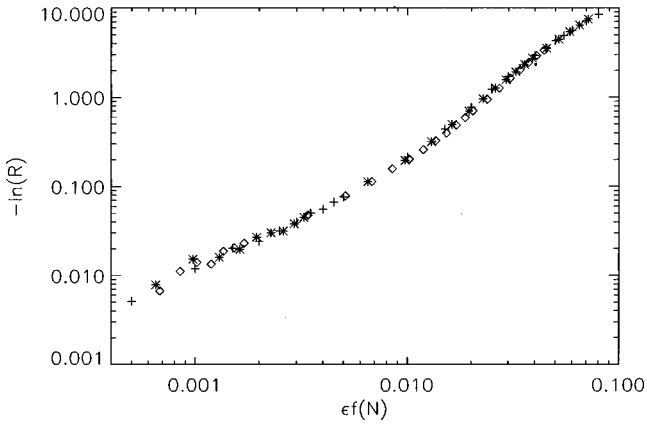

FIG. 14. The curves shown in Fig. 13 can be shifted to overlap by changing the x axis from ϵ to $\epsilon f(N)$, where $f(N)$ is a function of the total number of particles in the system. $f(100)=1$. Three curves are shown, they are all for low density systems with Boltzmann boundary conditions. + is for $N=100$, * is for $N=70$, and ◇ is for $N=40$.

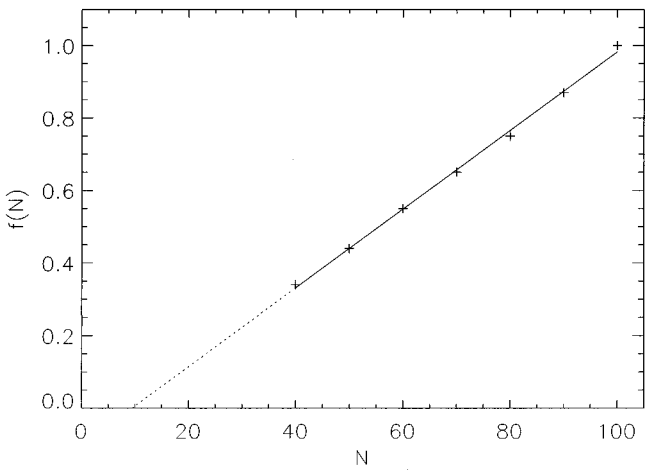

FIG. 15. The function $f(N)$ from Fig. 14. $f(N)$ is proportional to N with a small adjustment due to boundary effects.

Characteristicly for granular systems, fluctuations are important at all scales, enhanced by the combined effects of momentum conservation and nonuniformity. Also, the separation between fluctuations and mean flow is quite nontrivial. The mean motion (correlated) and the fluctuations relative to it have to be separated strictly speaking at every instant of time and at any position. Ideally, the fluctuations should be uncorrelated. But if the mean flow is an average of a collection of particles, the correlations between the fluctuations depend on the size of the collection.

An important issue is the existence of a universal description, which is not common for nonequilibrium systems. The separation of the dynamics into motion in the center of mass frame and the motion of the center of mass itself is quite suggestive.

The motion of the center of mass cannot be universal. Momentum conservation decides that the velocity of the center of mass can be changed only by interaction between particles and external effects. So it depends sensitively on the details of boundary conditions, as shown in this paper, and cannot be universal.

This is true for both elastic systems and inelastic ones. However, in elastic systems, every mode has the same strength due to the equipartition law of the energy. The motion of the center of mass is just one mode out of Nd modes, and its effect is negligible for a macroscopic system. In a dissipative system, on the other hand, being the only conserved mode, it can dominate over all other modes. Consequently, a universal description does not exist for the dynamics as a whole.

Still, if we look at the other $N-1$ modes which are perpendicular to this nonuniversal mode, we may discover some universal features. The independence of the motion in the center of mass frame on the boundary conditions and system sizes is a hint that this part of the dynamics may be universal. Further study is being carried out.

The thin pipe model used here greatly simplifies both the numerical and analytical calculations. The low density version of it may not have higher-dimensional analogies, where the sequence of particles is necessarily broken. However, the high density version can be modified for a higher-dimensional situation, where the sequence can be kept.

ACKNOWLEDGMENTS

This work is a continuation of the endeavor to understand the dynamics of granular systems carried out in the Chicago group led by Professor Leo Kadanoff. Professor Kadanoff formulated the pipe model as a nontrivial extension to the one-dimensional model. I want to thank him for his continuous help and encouragement during this work. I am also grateful to E. Ben-Naim and D. Rothman for interesting discussions. This work was supported by the National Science Foundation under Grant No. DMR-9415604, and in part by the MRSEC Program of the NSF under Grant No. DMR-9400379.

[1] A. Goldshtein and M. Shapiro, J. Fluid Mech. **282**, 75 (1995); A. Goldshtein, M. Shapiro, L. Moldavsky, and M. Fichman, *ibid.* **287**, 349 (1995); A. Goldshtein, M. Shapiro, and C. Gutfinger, *ibid.* **316**, 29 (1996); **327**, 117 (1996).
[2] E. L. Grossman and B. Roman, Phys. Fluids **8**, 3218 (1996).
[3] J. J. Brey, J. W. Dufty, and A. Santos, J. Stat. Phys. **87**, 1051 (1997); J. W. Dufty, J. J. Brey, and A. Santos, Physica A **240**, 212 (1997).
[4] J. J. Brey and D. Cubero, Phys. Rev. E **57**, 2019 (1998).
[5] T. P. C. van Noije and M. H. Ernst, e-print cond-mat/9803042.
[6] P. K. Haff, J. Fluid Mech. **134**, 401 (1983).
[7] J. T. Jenkins and S. B. Savage, J. Fluid Mech. **134**, 187 (1983).
[8] J. T. Jenkins and M. W. Richman, J. Fluid Mech. **192**, 313 (1988).
[9] J. T. Jenkins, J. Appl. Mech. **59**, 120 (1992).
[10] H. Hayakawa, S. Yue, and D. C. Hong, Phys. Rev. Lett. **75**, 2328 (1995).
[11] N. Sela and I. Goldhirsch, Phys. Fluids **7**, 507 (1996).
[12] E. L. Grossman, T. Zhou, and E. Ben-Naim, Phys. Rev. E **55**, 4200 (1997).
[13] S. McNamara and S. Luding, e-print cond-mat/9805257.
[14] S. Luding, M. Huthmann, S. McNamara, and A. Zippelius, e-print cond-mat/9804003.
[15] S. Luding, M. Müller, and S. McNamara (unpublished).
[16] T. P. C. van Noije, M. H. Ernst, and T. Brito, e-print cond-mat/9710102.
[17] T. Zhou, Phys. Rev. Lett. **80**, 3755 (1998).
[18] F. Melo, P. B. Umbanhower, and H. L. Swinney, Phys. Rev. Lett. **75**, 3838 (1995); T. Metcalf, J. B. Knight, and H. M. Jaeger, Physica A **236**, 202 (1997).
[19] J. B. Knight, H. M. Jaeger, and S. R. Nagel, Phys. Rev. Lett. **70**, 3728 (1993).
[20] H. M. Jaeger, S. R. Nagel, and R. P. Behringer, Rev. Mod. Phys. **68**, 1259 (1996).
[21] I. Goldhirsch and G. Zanetti, Phys. Rev. Lett. **70**, 1619 (1993).
[22] M. Y. Louge, J. T. Jenkins, and M. A. Hopkins, Mech. Mater. **16**, 199 (1993).
[23] Y. Du, H. Li, and L. P. Kadanoff, Phys. Rev. Lett. **74**, 1268 (1995).
[24] T. Pöschel, J. Phys. (France) **4**, 499 (1994).
[25] Along with many others, this observation is due to Leo Kadanoff's insight.